Springer

Journal of Mechanical Science and Technology 22 (2008) 2454~2463

Journal of Mechanical Science and Technology

www.springerlink.com/content/1738-494x
DOI 10.1007/s12206-008-0713-1

Investigation of cutting characteristics for worm machining on automatic lathe – Comparison of planetary milling and side milling †

MinHwan Lee[1], DongBae Kang[2], SeongMin Son[3,*] and JungHwan Ahn[2]

[1]*Global R&D H.Q., Mando Corporation, Giheung-Gu, Yongin-Si, Kyonggi-Do 446-901, Korea*
[2]*School of Mechanical Engineering, Pusan National University, JangJeon-Dong, Busan 609-735, Korea*
[3] *School of Mechanical Engineering, Ulsan College, MuGeo2-Dong, Nam-Gu, Ulsan 680-749, Korea*

(Manuscript Received December 12, 2007; Revised July 15, 2008; Accepted July 16, 2008)

Abstract

A worm and worm wheel gearing is widely used in a geared motor unit for the convenience and safety of an automobile. For mass production of a high quality worm, the current rolling process is substituted with the milling process. The milling process offers comparatively accurate machining quality and high production capacity for worm manufacturing. Moreover, since the milling process enables the integration of all operations of worm manufacturing on a CNC lathe, production efficiency can be remarkably improved. However, there are several important factors to be considered for producing high quality worms such as cutting force, tool-workpiece interference, and others. Planetary milling and side milling are generally applied to machine worms. In this study, the cutting characteristics of worm machining on an automatic lathe are investigated for two types of milling processes and those processes are compared with each other. A tool-tip trajectory model based on tool-workpiece interaction is proposed, and then tool-workpiece interference and cutting force are simulated with the model. The simulation results are verified through numerous experiments. The experimental results show the cutting characteristics of each milling process and the efficiency for mass production of a high quality worm.

Keywords: Worm; Planetary milling; Side milling

1. Introduction

A worm and worm wheel gearing is widely used in geared motor units for automobile convenience and safety. A worm gear is a compact power transmission mechanism which substantially decreases speed and increases torque. Fig. 1 shows the structure of a driving system of a worm gearing in an automotive DC motor. Fig. 1(a) is the structure of an electric adjusting pedal. The DC motor rotates a worm, and then the power is transmitted to rotate a worm wheel and a nut attached to the worm wheel. Finally, linear movement is generated through a nut-lead screw mechanism to adjust the pedal height. Fig. 1(b) is the structure of a deployable running board motor, which has two pairs of worm gear sets to generate high torque and reduce gear sound. Since the second worm is inserted into the first worm wheel, the torque converted at the first gear set is converted again at the second gear set. This kind of gear mechanism generally produces a good sound performance compared to other similar gear reduction mechanisms.

For mass production, worms have been typically manufactured by roll forming. Although the residual stress caused by plastic forming in the thread rolling process increases the fatigue life of machined components, roll formed worms have problems of accuracy due to the difficulty of controlling residual stresses,

† This paper was recommended for publication in revised form by Associate Editor Dae-Eun Kim

*Corresponding author. Tel.: +82 52 279 3104, Fax.: +82 52 279 3137
E-mail address: semson@mail.uc.ac.kr

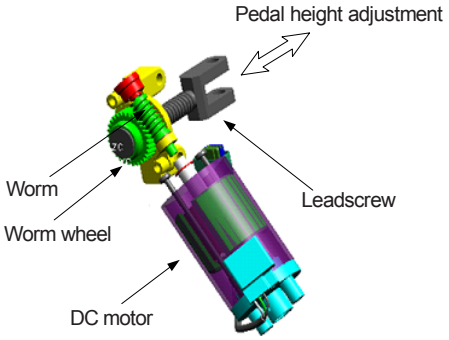

(a) Pedal adjusting motor

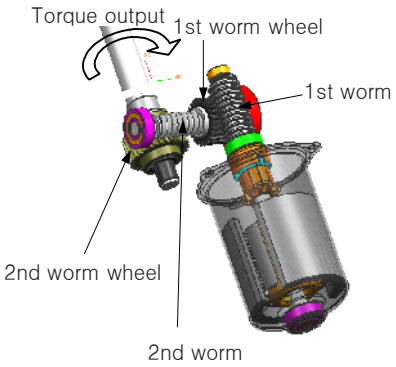

(b) Deployable running board motor

Fig. 1. Structure of worm geared DC motor.

and those cause noise and inadequate performance as worms are driven. An automobile's convenience and safety unit must show high performance and have low noise as desired by customers. For this reason, worm production by milling is substituting that by rolling. The milling process offers comparatively accurate machining quality and high production capacity of worms. Moreover, since milling enables the integration of all operations of worm manufacturing on a CNC lathe, production efficiency can be remarkably improved. But conventional milling tools are not suitable for such integration on a CNC lathe because of their large sizes and complicated power transmission mechanism. So most milling machines for thread cutting have been manufactured as an independent machine of special purpose.

Planetary milling and side milling are generally applied to a machine worm for mass production. These methods use a number of tool bites, which are installed on the outer race or inner race of a tool holder ring. Mohan and Shunmungam studied tool interference and profiling in worm machining by simulation

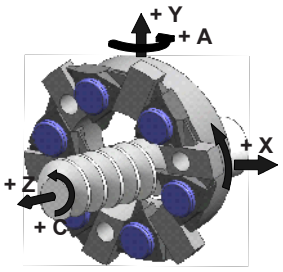

(a) Three dimensional view

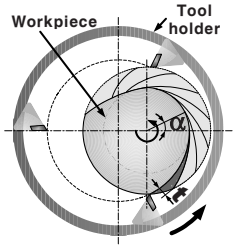

(b) Chip generation mechanism

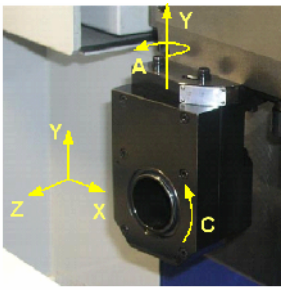

(c) Photograph of tool

Fig. 2. Mechanism of planetary milling.

and analyzed them mathematically with a transformation matrix [1, 2]. Feng and Tsay proposed a mathematical model according to worm type to analyze the mechanism of worm gear manufacturing with a hob-cutter [3, 4]. Etheridge geometrically analyzed the interference due to tool shape during the helical slot milling using the disc type cutter [5].

In this study, a mathematical model is proposed to calculate the tool-tip trajectories of a planetary milling cutter and side milling cutter, which are specially designed to be integrated on an automatic lathe. Based on the model, cutting force is simulated theoretically by considering machining conditions such as tool speed and feed rate. In addition, tool-tip interference is also simulated with experimental conditions and analyzed through experiments. Then, the characteristics of these machining processes are investigated by comparison of simulations and experimental results.

2. Cutting mechanism of planetary milling and side milling

2.1 Planetary milling

Planetary milling (whirling process) is a machining process in which a series of tool tips removes material by passing over the rotating workpiece and advancing at lead to produce a helical form. Fig. 2 shows the schematics of the cutting mechanism of planetary milling and the chip generation mechanism. Tool tips are arranged along the inside of the tool holder. The tool holder is tilted to the nominal helix angle of the worm. Threads of a worm are generated as a result of the tool holder rotating at high speed around a slowly rotating workpiece. The rotating workpiece proceeds along the longitudinal direction and produces the designed pitch of the worm. The eccentricity of the worm centerline to the tool holder ring determines the height of the thread.

Since smaller cusp and longer cutting chip are generated by planetary milling as shown in Fig. 2(b), the quality of the machined surface is expected to improve, and the cutting load for each tool tip is alleviated [6]. But because the number of tool tips attached on the inside of a tool holder is relatively fewer than that of side milling, it is difficult to increase the rotating speed of the milling cutter. The interference between the milling cutter and the worm thread surface during the milling of a large helix angle is also unavoidable due to geometrical limits of planetary milling.

2.2 Side milling

Fig. 3 shows a schematic for the cutting mechanism of side milling and the chip generation mechanism. The milling cutter rotating at high speed produces threads on the slowly rotating workpiece. Side milling process also uses a cutter with a series of tool tips attached on a tool holder ring. Since the tool tips are arranged along the outside of the tool holder, the tool holder can attach more tool tips than the case of planetary milling for the same size of the tool holder ring. Therefore, the cutting force is extensively distributed to the increased number of tool tips, and this enables the cutter rotating speed to be increased highly. The height of cusp might be a problem if the rotating speed of the milling cutter is not sufficiently high.

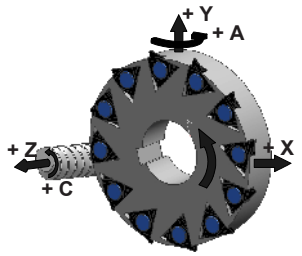

(a) Three dimensional view

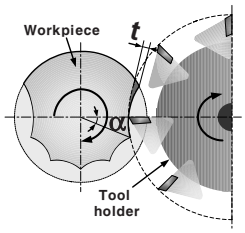

(b) Chip generation mechanism

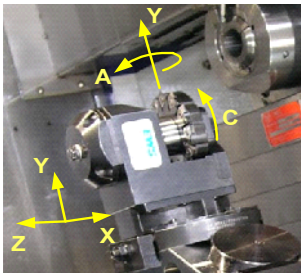

(c) Photograph of tool

Fig. 3. Mechanism of side milling.

Compared to planetary milling, a side milling cutter does not enclose a workpiece, and so the interference between the milling cutter and the worm thread surface during the machining of a large helix angle is not a serious problem.

2.3 Mathematical model of tool trajectory

Tool trajectory modeling is used to understand the worm geometry. Fig. 4 illustrates the tool-workpiece interaction in worm thread machining by planetary milling and side milling. The tool tip trajectory in the tool coordinate system is transformed into the trajectory in workpiece coordinates by Eq. (1) considering tool rotation, helix angle rotation, and translation, which is the tool offset and tool feed. The tool axis is offset by l from the workpiece axis and swiveled to the thread helix angle β. The tool coordinates (X_T, Y_T, Z_T) and the workpiece coordinates (X_W, Y_W, Z_W) are related by a transformation matrix **H**.

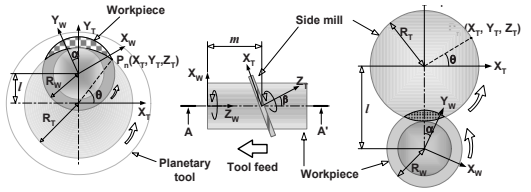

(a) Planetary milling (b) Side milling

θ : Angular position of the nth tool tip, α : Rotational angle of workpiece, β : Thread helix angle

Fig. 4. Tool-workpiece interaction in planetary milling and side milling.

$$\mathbf{H} = \mathbf{R}_1\mathbf{T}\mathbf{R}_2 \tag{1}$$

where **H**, $\mathbf{R_1}$, **T**, and $\mathbf{R_2}$ are expressed as follows:

$$\mathbf{R}_1 = \begin{bmatrix} \cos\alpha & -\sin\alpha & 0 & 0 \\ \sin\alpha & \cos\alpha & 0 & 0 \\ 0 & 0 & 1 & 0 \\ 0 & 0 & 0 & 1 \end{bmatrix} \quad \mathbf{T} = \begin{bmatrix} 1 & 0 & 0 & 0 \\ 0 & 1 & 0 & l \\ 0 & 0 & 1 & m \\ 0 & 0 & 0 & 1 \end{bmatrix}$$

$$\mathbf{R}_2 = \begin{bmatrix} \cos\beta & 0 & \sin\beta & 0 \\ 0 & 1 & 0 & 0 \\ -\sin\beta & 0 & \cos\beta & 0 \\ 0 & 0 & 0 & 1 \end{bmatrix}$$

$$\mathbf{H} = \begin{bmatrix} \cos\alpha\cdot\cos\beta & -\sin\alpha & \cos\alpha\cdot\sin\beta & -l\cdot\sin\alpha \\ \sin\alpha\cdot\cos\beta & \cos\alpha & \sin\alpha\cdot\sin\beta & l\cdot\cos\alpha \\ -\sin\beta & 0 & \cos\beta & m \\ 0 & 0 & 0 & 0 \end{bmatrix}$$

In the expression, $\mathbf{R_1}$, **T**, and $\mathbf{R_2}$ are transformation matrices for workpiece rotation α, tool offset l and tool feed m, and thread helix angle β, respectively. After being transformed by **H**, the position of the n-th tip, $P_n(X_T, Y_T, Z_T, 1)^T$, at angle θ on the cutter is expressed in workpiece coordinates as follows:

$$[P_n(X_W,Y_W,Z_W,1)]^T = \mathbf{H}[P_n(X_T,Y_T,Z_T,1)]^T$$
$$= \begin{bmatrix} X_T\cdot\cos\alpha\cdot\cos\beta - Y_T\cdot\sin\alpha + Z_T\cdot\cos\alpha\cdot\sin\beta - l\cdot\sin\alpha \\ X_T\cdot\sin\alpha\cdot\cos\beta + Y_T\cdot\cos\alpha + Z_T\cdot\sin\alpha\cdot\sin\beta + l\cdot\cos\alpha \\ -X_T\cdot\sin\beta + Z_T\cdot\cos\beta + m \\ 1 \end{bmatrix} \tag{2}$$

In this way, all of the trajectories of tool tips according to the tool rotational speed and feedrate can be calculated on the workpiece. In real cutting, the tool offset varies with each tip because the run-out of

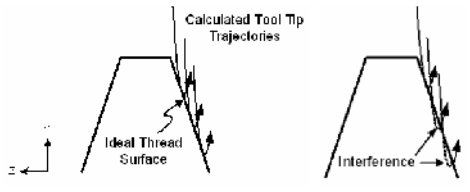

(a) Thread cutting without interference (b) Thread cutting with interference

Fig. 5. Definition of tool interference.

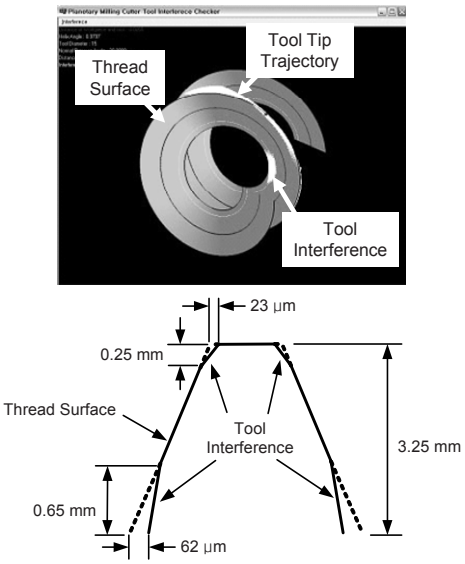

(a) Planetary milling

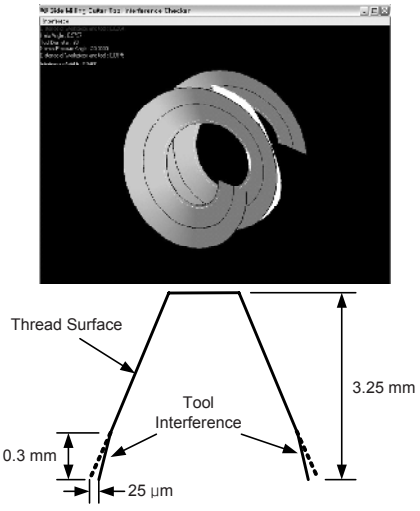

(b) Side milling

Fig. 6. Tool interference results according to worm and cutter parameter.

Table 1. Worm specification for simulation and experiment.

Module	Helix angle (deg)	No. of start	Pressure angle (deg)	Lead (mm)	Pitch Diameter (mm)
1.5	8.98°	1	20°	4.77	9.61

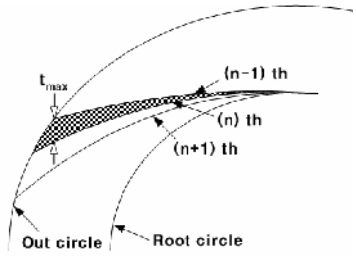

(a) Tool tip trajectory in cross-section of workpiece

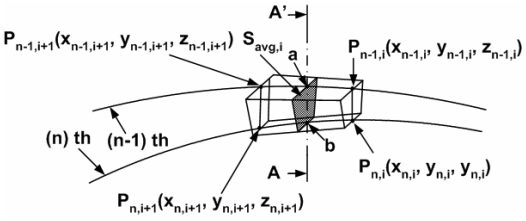

(b) Infinitesimal cutting volume

Fig. 7. Tool trajectory and cutting volume of the planetary milling.

tool axis and the setup error of tool tip are differently superimposed to the nominal value depending on the tip position.

2.4 Simulation of tool interference

A cutting simulation based on the mathematical model of tool trajectory was carried out to investigate the interference between the milling cutter and the worm thread surface. The interference of tool trajectory and thread surface is defined as Fig. 5. When the calculated tool trajectory intrudes the border line of the ideal thread surface, the tool tip interferes with the thread surface at the position. Table 1 is the specification of the simulated worm thread, and Fig. 6 shows the simulated results for planetary milling and side milling. In the 3D results, the gray area is the designed thread surface and the white area is the trajectory of the tool tips. The thread surface is partially overlapped by the tool trajectory due to the interference of the tool tips and threads. The interference area is spread not only on the root but also on the crest of

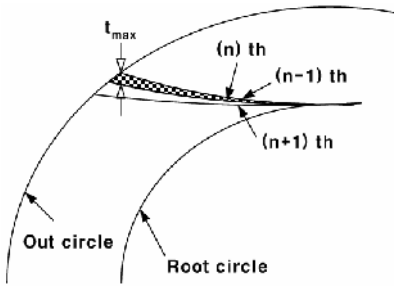

(a) Tool tip trajectory in cross-section of workpiece

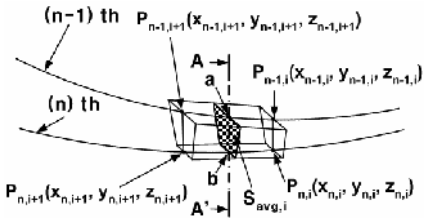

(b) Infinitesimal cutting volume

Fig. 8. Tool trajectory and cutting volume of the side milling.

the threads in the case of planetary milling. On the contrary, interference appears slightly only in the thread root in side milling. The line drawings in Fig. 6 show the generated thread surface with interference in axial section and the detailed interference.

From the simulation results, it appears that side milling generates less interference of milling cutter-thread surface and low cutting force. Therefore, it can be expected that the worm produced by side milling has geometrical accuracy and higher material quality.

2.5 Simulation of cutting force

Fig. 7 and Fig. 8 explain the infinitesimal cutting volume and the tool tip trajectory to calculate a cutting force of planetary milling and side miling. Fig. 7(a) and Fig. 8(a) are the trajectories in the x-y plane of the workpiece, which is generated by (n-1), n, and (n+1)-th tool tips of both milling cutters. In the figure, the chip become the thickest geometically at outside diameter. And Fig. 7(b) and Fig. 8(b) are infinitesimal volume to be cut out by a tool tip. The infinitesimal volume is defined with the section of trapezoid tool tip with pressure angle and the neighboring two trajectories generated by n and (n-1)-th tool tips. Then, the infinitesimal volume can be simlified using the average length of the two trajectories $L_{avg,i}$ and the average tool tip area $S_{avg,i}$. Therefore, the volume to be removed as chip by n-th tool tip is formulated as

Eq. (3).

$$V_n = \sum_{i=0}^{m} S_i(\theta_n, \theta_{n-1}) L_i(\theta_n) = \sum_{i=0}^{m} S_{avg,i} L_{avg,i} \tag{3}$$

Fig. 9 is a section to be defined by the trajectories of n and (n-1)-th tool tip. The width W_0 is the start point of machining and the width W_i varies according to the gap of two trajectories. The width W_i can be expressed by the width W_0, the pressure angle φ, and the distance $h_{avg,i}$ between two trajectories. Therefore, the average tool tip area $S_{avg,i}$ is expressed as follows:

$$S_{avg,i} = W_0 h_{avg,i} + (\tan\phi) h_{avg,i}^2 \tag{4}$$

$$h_{avg,i} = \overline{ab} = \frac{\overline{P_{n,i}P_{n-1,i}} + \overline{P_{n,i+1}P_{n-1,i+1}}}{2}$$

Using the trajectory coordinate of the infinitesimal volume in Fig. 7 and Fig. 8, the average volume length $L_{avg,i}$ can be written as Eq. (5).

$$L_{avg,i} = \frac{\overline{P_{n,i}P_{n,i+1}} + \overline{P_{n-1,i}P_{n-1,i+1}}}{2} \tag{5}$$

From Eqs. (3), (4), and (5), the cutting volume is proportional to the average tool tip area $S_{avg,i}$ and the average length $L_{avg,i}$. $S_{avg,i}$ is proportional to the distance between n and (n-1)-th tool tip trajectory. In the relation between volume parameters and cutting parameters, $L_{avg,i}$ is proportional to feedrate and tool diameter, and $h_{avg,i}$ is inversely proportional to the number of tool tips and tool rotational speed. In addition, $h_{avg,i}$ is proportional to feedrate.

Fig. 10 shows the simulated removal volume per revolution by planetary milling and side milling under the same machining conditions with experiments. The removal volume for each tool tip by side milling is less than that by planetary milling under the same feedrate. Therefore, the cutting speed of side milling can be set as higher than the case of planetary milling, because the cutting force per tool tip in side milling is much smaller than that in planetary milling.

$$U_m = F \cdot v = u_m \cdot MRR$$

$$F = \frac{u_m}{\Delta l} \cdot \Delta V = c_m \cdot \Delta V \tag{6}$$

U_m : specific cutting energy
F : cutting force
v : cutting speed
Δl : unit cutting length,
c_m : specific cutting energy for unit cutting length
ΔV : unit cutting volume

In this study, cutting forces for both milling types were estimated by calculating cutting volume and measuring specific cutting energy. Cutting force (F) can be acquired from specific cutting energy and unit cutting volume as Eq. (6). The specific cutting force for unit cutting length (c_m) is determined by tool tip

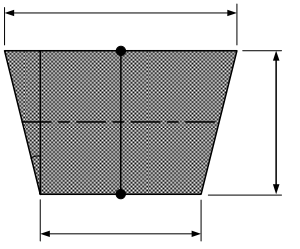

Fig. 9. Tool tip section in two neighboring tip trajectories.

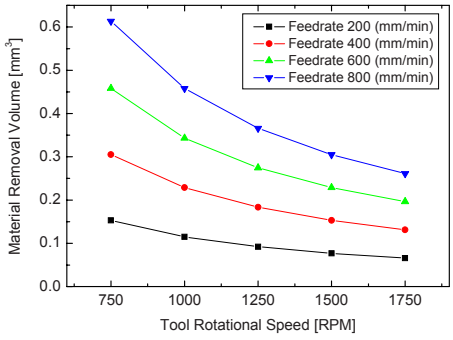

(a) Planetary milling

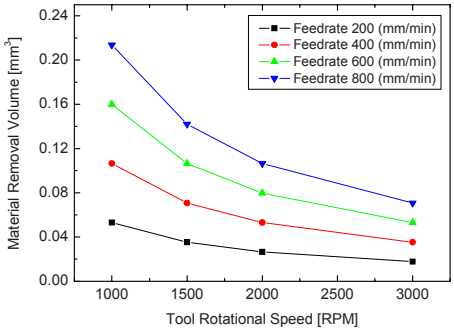

(b) Side milling

Fig. 10. Simulated cutting volume.

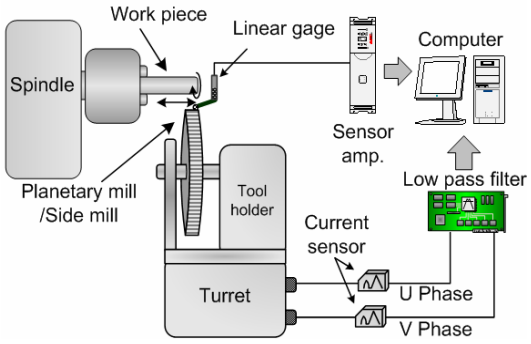

Fig. 11. Apparatus of the machining experiment on automatic CNC lathe.

trajectory of the milling process and the resultant cutting force acquired from experiments. The reason why the cutting force was calculated with material removal volume is due to variable cutting thickness on the tool trajectory. The calculation with cutting volume is easier than that with cutting area, and is able to be directly compared with experimental value from the current sensor which was used to get cutting force from the rotational tool.

For cutting force simulation, the cutting volume was derived from the mathematical model described above, and the specific cutting energy was acquired from a machining experiment on an automatic CNC lathe with the equipment schematized as Fig. 11. In planetary milling, the range of the tool rotation speed is less than that of side milling because of the motor driving method using a reducer. Fig. 12 is the result of cutting force conversion from material removal volume with specific cutting energy. As shown in Fig. 12, the cutting force for side milling is also much less than that of planetary milling under the same machining condition. This is due to the difference in the cutting volume per tool tip between the two milling types.

For a worm which has small module and small helix angle, planetary milling has high quality of thread surface because the stiffness of the inscribed tool mechanism is relatively high and the geometrical improvement in surface roughness is excellent. On the other hand, since the producible types of worms by planetary milling are limited and the cutting force for each tool tip is relatively high, the range of feedrate and tool rotational speed are restricted within narrow limits. However, side milling is free from the limitation of producible worm types and the surface roughness is able to be improved by increasing tool

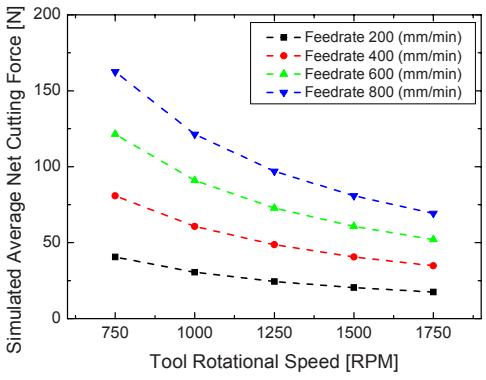

(a) Planetary milling

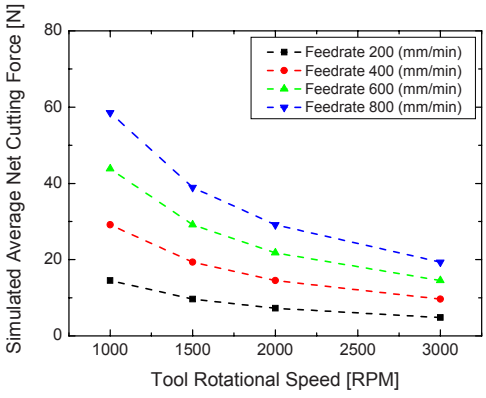

(b) Side milling

Fig. 12. Estimated cutting force.

rotational speed. The feedrate and the tool rotational speed can be operated in a variety of ways owing to smaller cutting force per tool tip than planetary milling.

3. Experimental results

3.1 Experimental conditions

Machining experiments were conducted on an automatic CNC lathe under several machining conditions as summarized in tables 2 and 3. The tool tip shape was same as the section of Fig. 9. During the experiments, cutting force was indirectly measured through current sensors, which were calibrated with reference to a dynamometer installed at a driving unit of the spindle. The dynamometer was a Kistler 9272A and the current sensor model was a Tektronix 622. The run out of tool tip was detected by a contact type linear gauge Mitutoyo 542-222 and the workpiece material was SUM24L as free cutting steel.

Table 2. Experimental conditions for worm machining.

Feed rate (mm/min)	Cutting depth (mm)	Tool speed (RPM)	
		Planetary milling	Side milling
200	3.25	750,1000,1250, 1500,1750	1000,1500,2000, 3000
400			
600			
800			

Table 3. Cutter parameter for worm machining.

	Diameter (mm)	Side angle of tool tip (deg.)	No. of bite	Nose radius (mm)	Height of tool tip (mm)
Planetary milling	15	20°	6	0.4	3.5
Side milling	80	20°	12	0.4	3.5

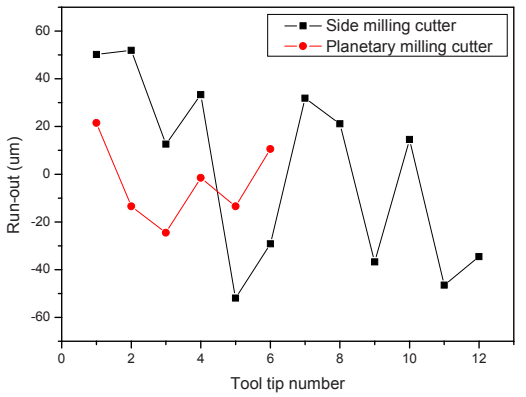

Fig. 13. Tool tip run-out of planetary milling cutter and side milling cutter.

3.2 Tool-tip run-out error

The run-out error of the tool tips mounted on milling cutter was investigated for one revolution. The numbers of tool tips are 6 in planetary milling and 12 in side milling, and Fig. 13 shows the measurement results. In the case of side milling, the run-out error varies up to 100 ㎛, which is twice as large as that of planetary milling. It is a disadvantage of side milling because the number of tool tips is more than that of planetary milling.

3.3 Cutting force

Fig. 14 shows the results of the measured cutting force for planetary milling and side milling, and the

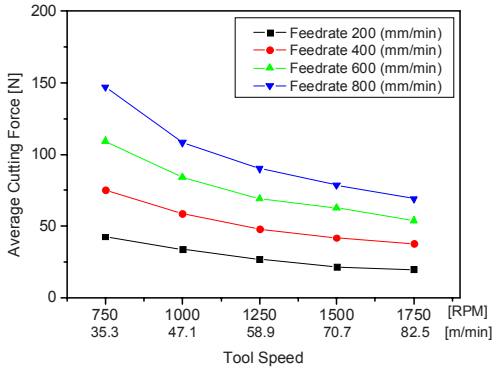

(a) Planetary milling

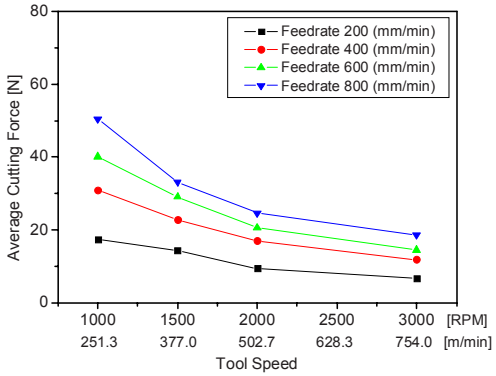

(b) Side milling

Fig. 14. Comparison of cutting force between planetary milling and side milling.

values are very similar to those of the simulation. Both patterns have almost the same decreasing trend with increasing tool rotational speed. In the case of planetary milling, the milling cutter on the automatic lathe is not driven directly by the motor but driven by the reduction gear, and the cutting force changes rapidly with the tool speed change. The application of a reducer for planetary milling makes a considerable cutting speed difference compared with side milling. Fig. 15 shows the linear velocities for planetary milling and side milling. In the case of planetary milling, the tool holder cannot have a diameter as wide as that of side milling, and the inner diameter of the planetary milling tool holder is commonly less than 20 ㎜. Since the milling tool holder should be rotated depending on helix angle, the size of the planetary milling tool holder is not so free as the side milling tool holder from interference between the tool holder and other materials such as workpiece and equipment on the machine tool. Therefore, planetary milling needs a

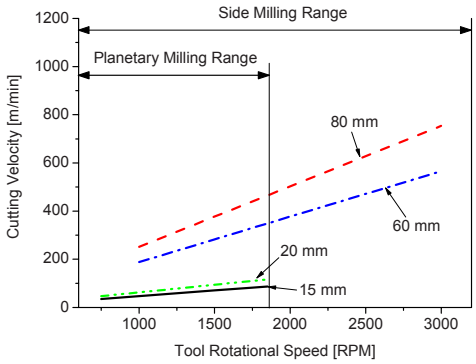

Fig. 15. Tool cutting velocity range according to tool diameter and rotational speed.

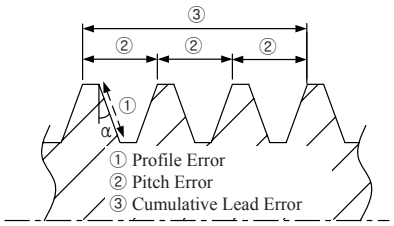

Fig. 16. Worm accuracy specification.

reducer in order to overcome the defect from relatively number of tool tips. The reducer performs two important functions in the cutting process. The one is the supplementation of the driving torque to overcome the high cutting force which the less number of tool tips causes. The other is the rotational speed reduction to prevent excessive wear of the tool tip by a high cutting force.

On the contrary, side milling can be applied up to higher cutting speed because the spindle torque is transmitted to the tool rotation without gear reduction. The increased cutting speed within the limit linear velocity of the tool tip reduces the cutting force for each tool tip and extends the tool life. The cutting forces of side milling are much less than those of planetary milling under the same feedrate as shown in Fig. 14. The cutting forces for side milling ranged from 6.7 N to 50.4 N, and those of planetary milling ranged from 19.7 N to 142.9 N.

3.4 Quality of machined thread

The accuracy of the machined worms by both milling processes was investigated. Fig. 16 illustrates the prescribed factors of thread to verify the worm accuracy, and table 4 presents the measurement results.

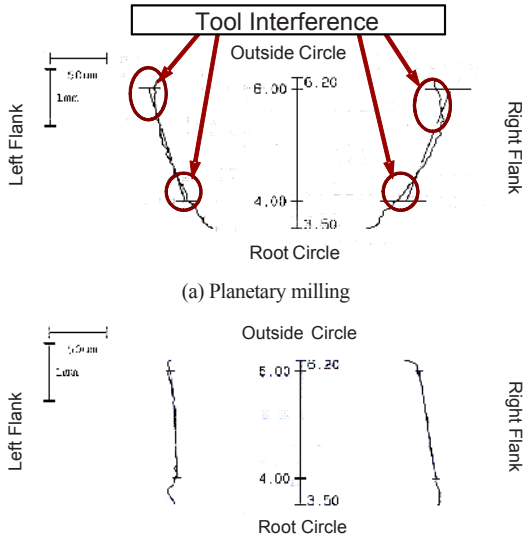

(a) Planetary milling

(b) Side milling

Fig. 17. Comparison of thread profile between planetary milling and side milling.

The prescribed factors include cumulative lead error, pitch error, profile error, and roughness of the thread surface [7, 8]. Although side milling has a larger run-out of the tool tips, it is superior to planetary milling for all the specifications and especially, strong in the profile error. Fig. 17 illustrates the pattern of the thread profile machined by each milling process. The profile is more accurate as it approaches the vertical. The profile error of planetary milling is larger than that of side milling because of geometric error from non-coincidence between the contact point of the tool-workpiece and the origin of the workpiece axis. The tool offset is compensated to eliminate the error, but the compensation is very difficult due to the spatial limit from the peculiar mechanism, in which the planetary milling cutter encloses the workpiece. The interference between the tool tip and the surface of the thread is also shown in Fig. 17. Planetary milling generates some interference at the outer and root diameters of the worm thread, as shown in the simulated result. However, interference does not appear in the thread produced by side milling.

3.5 Cycle time of machining thread

The cycle time including threading time was investigated to compare productivities by roll forming and both milling methods. In the threading time, roll forming is superior to both milling methods as shown

Table 4. Threading time and quality for the milling methods.

	Planetary milling	Side milling
Profile Error (㎛)	22.1	15.7
Cumulative Lead Error (㎛)	8.6	7.5
Pitch Error (㎛)	4	3.2
Thread Surface (R_{max}-㎛)	6.34	5.887
Threading Time (sec)	36	28
Tool Speed (RPM)	1900	1800

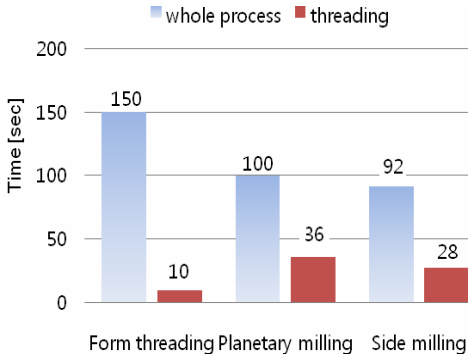

Fig. 18. Cycle time according to worm manufacturing method.

in Fig. 18. The times are 10 sec, 28 sec, and 36 sec, respectively, for roll forming, side milling, and planetary milling. By side milling, however, the cycle time of a worm gear is the shortest as 92 sec. Worm gear generation by the two milling methods can be integrated with an automatic CNC lathe, but roll forming generates a worm gear through several processes with two separated machines. The difference of cycle time between the two milling methods is 8 sec from the difference of threading time. Therefore, the productivity improvement by application of side milling can be expected as 8.7% and 63%, respectively, compared to planetary milling and roll forming.

4. Conclusion

The cutting characteristics for worm machining on an automatic lathe were investigated theoretically and experimentally. Following conclusions have been drawn:

(1) A tool-tip trajectory model based on a tool-workpiece interaction was derived in terms of matrix transformation, and the tool-workpiece interference and cutting force were simulated with the model. The tool-tip trajectory model was verified through a comparison of simulation and experiment.

(2) In the case of planetary milling, the relatively fewer tool tips requires not only increasing the driving torque but also reducing the driving speed by using a reducer to supplement cutting force and prevent excessive tool tip wear from a high cutting force. On the contrary, side milling can be applied up to higher cutting speed and the cutting force is less than half of that in planetary milling under the same feedrate.

(3) Side milling is superior to planetary milling for the described factors such as threading time, cumulative lead error, and profile error. Moreover, the interference between the tool tips and the surface of the thread does not appear in the thread produced by side milling.

References

[1] L. V. Mohan and M. S. Shunmungam, Simulation of whirling process and tool profiling for machining of worms, J. Mater. Process. Technol. (185) (2007) 191-197.

[2] L. V. Mohan and M. S. Shunmungam, CAD approach for simulation of generation machining and identification of contact lines, Int. J. Mach. Tools Manuf. (44) (2004) 717-723.

[3] H. S. Feng and C. B. Tsay, Mathematical model and bearing contacts of the ZK-type worm gear set cut by oversize hob cutters, Mech. Mach. Theory 31 (3) (1996) 271-282.

[4] C. B. Tsay, J. W. Jeng and H. S. Feng, A mathematical model of the ZE-Type worm gear set, Mech. Mach. Theory 30 (6) (1995) 777-789.

[5] R. A. Etheridge, An analysis of the interference produced when milling a helical slot with disc type cutters, Int. J. Mach. Tool Des. Res. (10) (1970) 143-157.

[6] R. Wehmanm, The Whirling Process for Improved Worm Gears, Gear Solutions Magazine, Alabama, USA, (2003).

[7] Klingelnberg, Worm software operating manual ver. 2.0, Klingelnberg GmbH, Hückeswagen, Germany, (2000).

[8] Germany standard, Concepts and parameters associated with cylindrical gears and cylindrical gear pairs with involute teeth, Germany, (1980).